A multicomponent, time-lapse investigation of fractures in a potash mining region.

Andrew Nicol* and Don Lawton

ABSTRACT

Time-lapse seismic analysis is used to monitor changes in the subsurface which occur in between the acquisition of the baseline and monitor surveys. In this study, the analysis of two multicomponent seismic vintages is conducted in order to monitor any fracture-induced changes to the seismic anisotropy in a potash mining region. The Dawson Bay Formation, a fractured carbonate which unconformably overlies the Prairie Evaporite Formation, which contains significant potash ore deposits, is the focus of this study. The two vintages of PP and PS volumes were divided into four sub-volumes consisting of a stack containing a 45 degree aperture of source-receiver ray paths. The azimuthal time difference plots created from the PP seismic data show travel-time differences running parallel to the edges of the highest density mine workings. Seismic interpretation and Vp/Vs analysis suggest that random fracturing is present in the subsurface, and is creating a significant low velocity anomaly observed as an increase in travel-time in the PP and PS volumes, while exhibiting a low amplitude effect in both vintages of the PP volumes.

INTRODUCTION

Multi-component, time-lapse seismic analysis in this study focuses on the anisotropic velocity changes associated with the fractured Devonian carbonate succession which unconformably overly a potash bearing Prairie Evaporite Formation. The potash deposits in the Elk Point Embayment (Figure 1) extend from the Northern United States (North Dakota) to the Northwest Territories (De Mille, Shouldice, & Nelson, 1964), and contain potash concentrations averaging between 20 and 30 percent K_2O making them some of the richest deposits in the world (Douglas, 1970; Mossop & Shetsen, 1993; Warren, 2006). The deposits lie 30 m below the top of the 100-200 m thick Prairie Evaporite Formation and are being extracted using the room and pillar method (Zhang, 2010).

Use of the room and pillar mining method, has the potential to alter the stress field in the subsurface which could re-activate fractures present due to paleo-stresses, or induce new fracturing. It is well understood that fractures impact of seismic imaging, and the propagation of fractures into the Dawson Bay Formation (a carbonate sequence which unconformably overlies the Prairie Evaporite Formation) could create a noticeable seismic anomalyin the 3-dimensional (3D) seismic volumes. Figure 2 displays a stratigraphic column for the region. Zhang (2010) assessed the feasibility for the detected of fractures using multi-component, time-lapse seismic methodology. He showed that P- and S-wave velocities will decrease significantly where fractures are present and an increase in event travel-time in both PP and PS synthetic seismograms. The seismic velocity variations can create different types of anisotropy in the Dawson Bay Formation depending on the existence of a preferential fracture orientation.
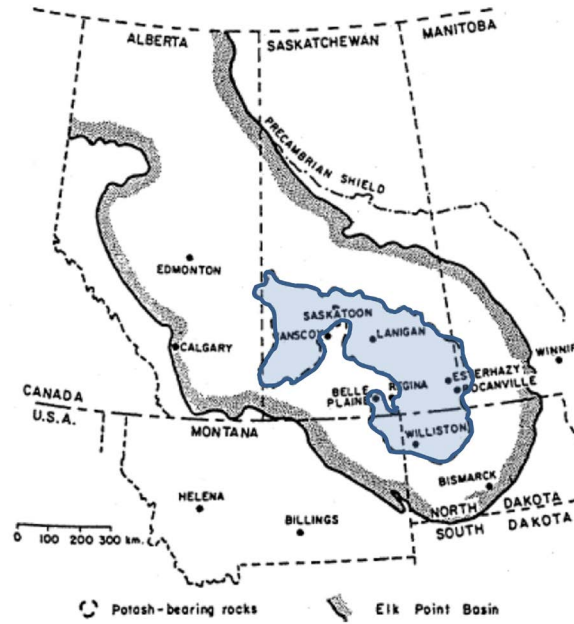
FIG. 1. A map of the Canadian Prairie Provinces showing the depositional limit of the potash bearing rocks (blue shaded area) within the Elk Point Basin(Fuzesy, 1982).
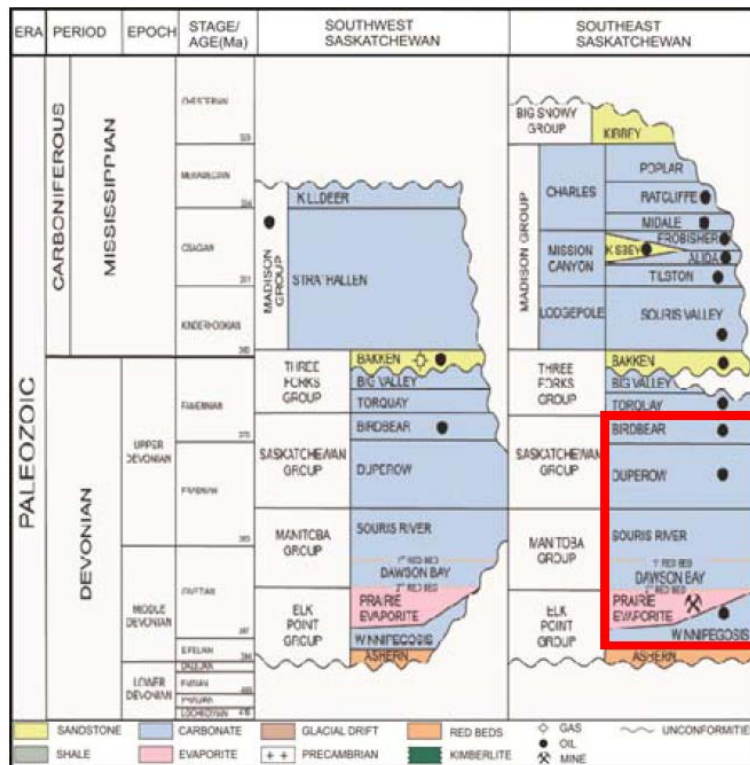

FIG. 2. A stratigraphic column for southeastern Saskatchewan showing the interval of interest highlighted in red.

AZIMUTHAL TRAVEL-TIME ANALYSIS

Fractures reduce the cohesion within the rock perpendicular to the direction of fracture propagation. Seismic waves propagating parallel to the fracture will not experience any change in velocity, whereas a seismic wave propagating perpendicular to the direction of fracture propagation will experience a decrease in velocity (Lynn, Beckham, Simon, Bates, Layman, & Jones, 1999; O'Connell & Budiansky, 1974; Ruger, 1997). Such velocity anomalies are referred to as transverse isotropy (Thomsen, 1986), and are more evident through the travel-time analysis of seismic events which travel at orthogonal source-receiver ray paths. In this study area, where fractures are 20-30 degrees subvertical (Boyd, 2012), and the surrounding carbonate stratigraphy is relatively flat, seismic waves are likely to experience a specific type of anisotropy called horizontal transverse isotropy, or HTI (Figure 3) (Hudson, 1981; Tsvankin, 1997).
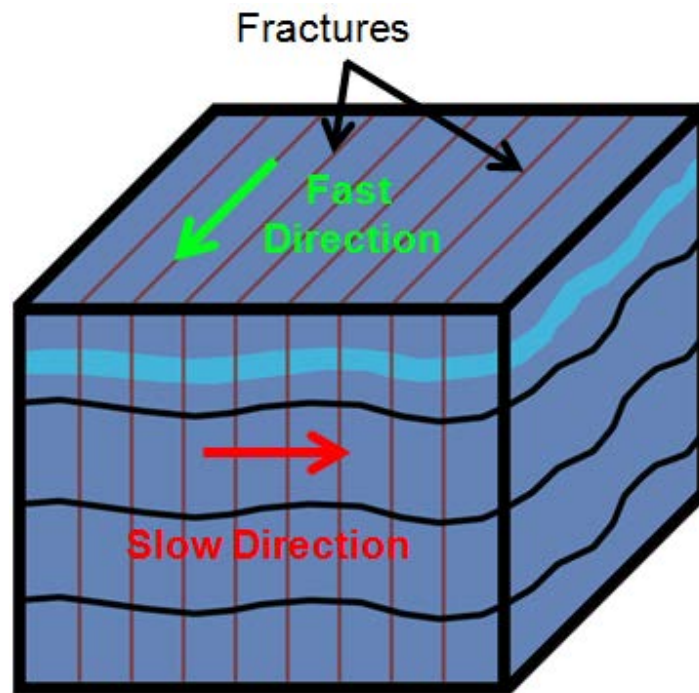

FIG. 3. Cartoon showing the fast and slow directions of seismic wave propagation with respect to fractures in the subsurface. The vertical fractures induce a reduction in seismic velocity perpendicular to the orientation of fracturing, where the seismic velocity parallel to fracturing is unchanged.

The presence of HTI allows for the analysis of travel-time differences between orthogonal azimuths. In order to do so, the PP and PS datasets were divided into 5 volumes; one full azimuth stack volumes and four azimuthally sectored volumes containing a stack encompassing a 45 degree aperture of reciprocal source-receiver ray paths. These volumes are centred around 0&180, 90&270, 45&225 and 135&335 (Figure 4). In order to detect possible HTI, five horizons were picked in each of the volumes: the Birdbear Formation, the Souris River Formation, the Dawson Bay Formation, the Prairie Evaporite Formation and the Winnipegosis Formation.

The effects of HTI induced from subsurface fracturing should be visible in the four sub-volumes due to the small changes in residual normal move-out (NMO) between azimuthal gathers using full-azimuth velocities. The changes in residual NMO propagate into the azimuthally sectored stacks and yield small travel-time differences in the stacked seismic events when the global NMO velocities are applied to the sectored volumes (Figure 5).

Travel-time differences were calculated by subtracting horizons picked from two orthogonal azimuthally sectored volumes centred around 0&180 and 90&270, called t_1 and t_3 respectively. Should the travel-time from t_1 be larger than that of t_3, the outcome is a positive time which would propose a slower seismic velocity in the 0&180 direction. A negative time suggests a slower seismic velocity in the 90&270 orientation. This process is then repeated for the 45&225 (t_2) and 135&335 (t_4) orientations.

Before travel-time differences can be calculated, seismic horizons were first tied to geological formations through the well tie process.
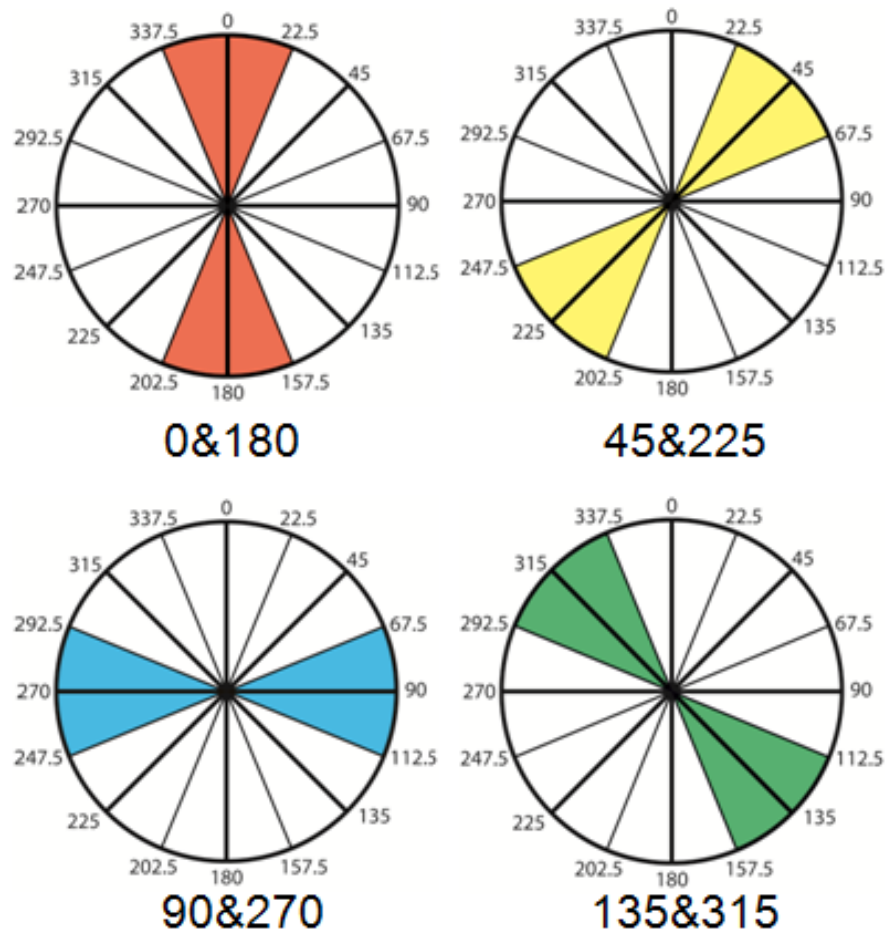

FIG. 4. Distribution of source-receiver ray paths used to make up the four azimuthally sectored seismic volumes. The volumes are labeled corresponding to the reciprocal azimuths in the middle of the stacked aperture.
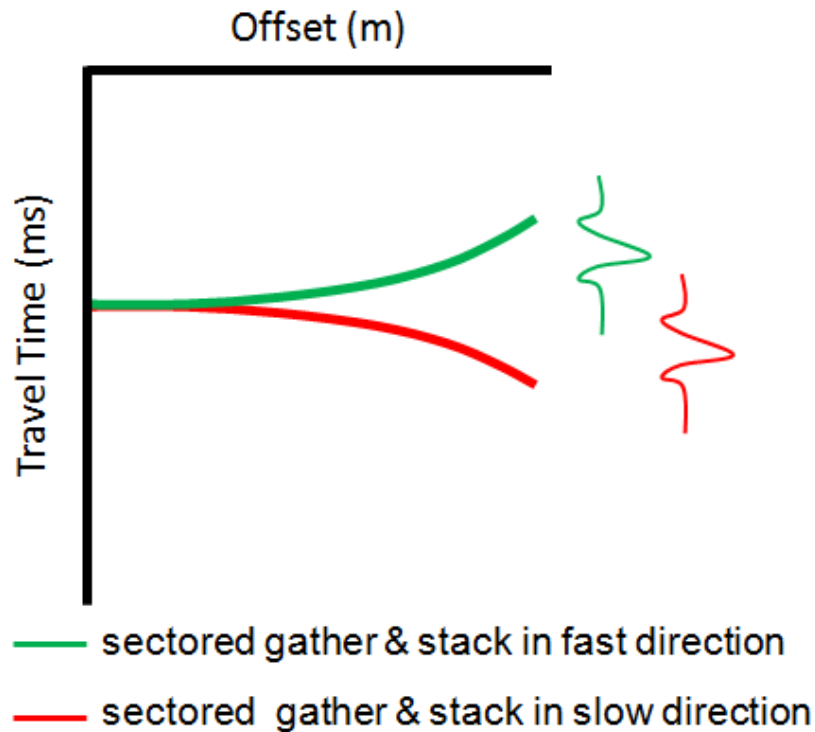
FIG. 5. The sectored receiver gathers and stacks corresponding to the directions of fast (green) and slow (red) seismic wave propagation, as well as the travel-times associated with those azimuthally sectored stacks.

Horizon Interpretation

In order to begin analysis of a seismic volume, the time subsurface formations were first correlated to the corresponding time on a seismic section. This is done through the generation of synthetic seismograms using P- and S- wave sonic and density wireline logs which are typically acquired when a well is drilled. In the study area there were 14 wells with P-wave sonic logs, 2 wells with dipole sonic logs, which provide the shear component, and 3 wells with density logs in the study area. Figure 6 shows blocked wireline logs from one of the wells used pick horizons on both the PP and PS data sets. The selection of seismic events which correspond to stratigraphic layers is crucial to the interpretation of a seismic dataset, and is accomplished by relating geological well tops to seismic reflectors through the generation of synthetic seismograms. The critical formations to the interpretation of this volume are the Birdbear Formation, the Souris River Formation, the Dawson Bay Formation, the Prairie Evaporite Formation and the Winnipegosis Formation, all of which are not shown on the log.
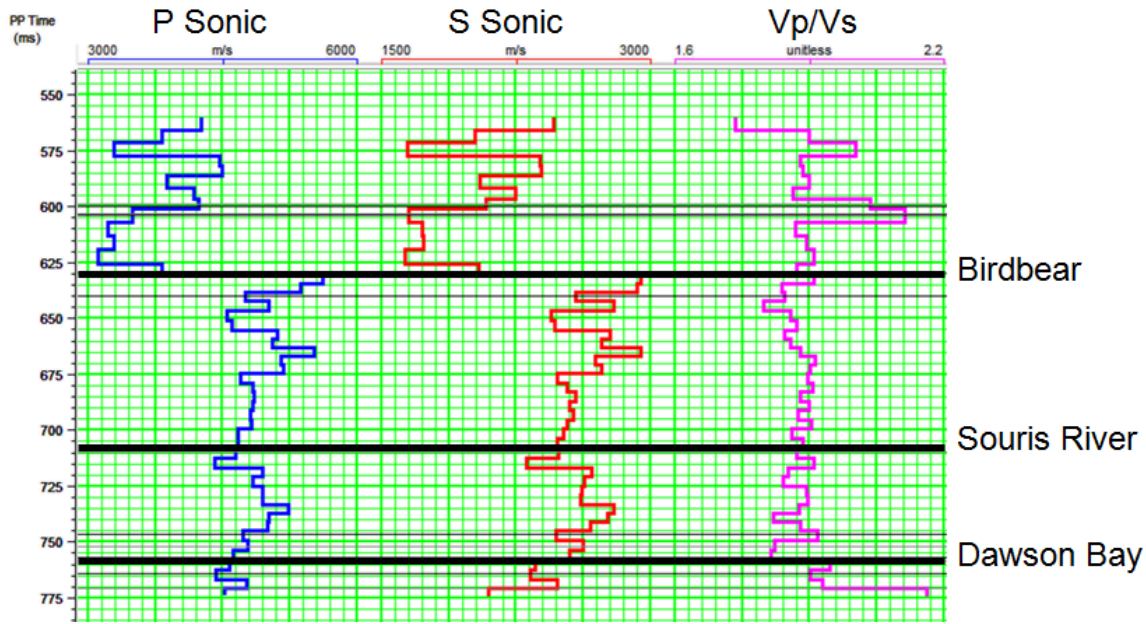
FIG. 6. Blocked wireline logs acquired from one of the wells in the study area. The p-wave sonic is in blue, s-wave sonic in red and the Vp/Vs calculated from both sonic logs in magenta. The geological tops are in black.

Correlation between the synthetic seismogram and the seismic volume is calculated at the well bore to insure an accurate assessment of the horizons to be interpreted. Figure 7 shows an example of a synthetic seismogram generated and its correlation, of 0.806, with the 2004 PP seismic volume. All 14 wells were tied in similar fashion and displayed similar correlation coefficients. The tying of the PS seismic is done using reflection coefficients calculated from both the p-wave and s-wave sonic logs, an additional step factors in the Vp/Vs to adjust the time-depth relationship accordingly. The two wells with dipole sonic wells were tied with only minute stretches applied to attain an optimal correlation of 0.685 (Figure 8).

The Prairie Evaporite and Winnipegosis formations are not seen as geological tops on the well logs in the area (Figures 6-8). This is because the wells are specifically planned not to penetrate the Prairie Evaporite Formation, and therefore were slightly more difficult to pick. The Prairie Evaporite Formation was picked in the PP seismic volumes based on the termination of the well log, and the location of the potash mine workings which are visible in the seismic volumes. The Winnipegosis Formation was picked in the baseline and monitor, PP and PS volumes through the identification of what are interpreted to be a carbonate mound in the Southeast and a pinnacle reef in the Northeast.
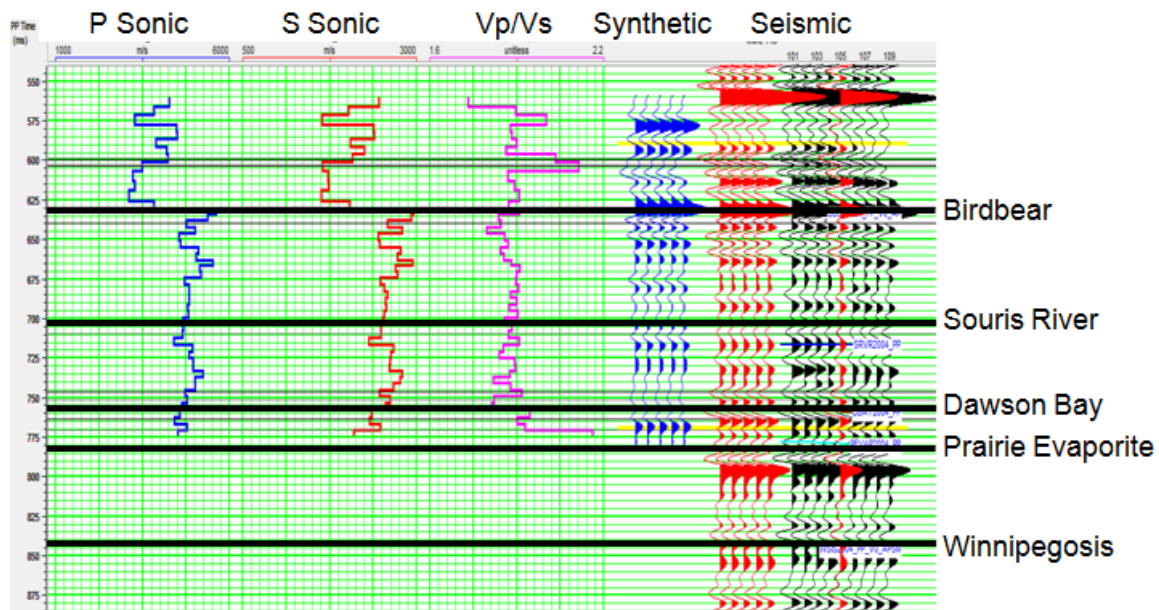
FIG. 7. Synthetic tie (blue seismic traces) constructed using the P-wave sonic (blue log) and is correlated with the 2004 PP seismic volume (red/black seismic traces).
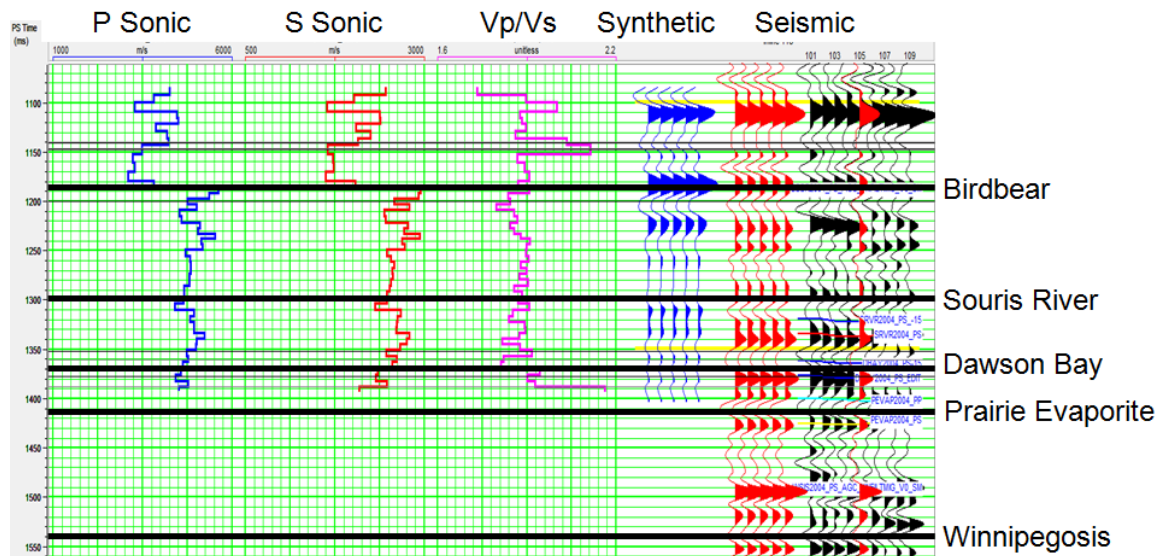

FIG. 8. Synthetic tie (blue seismic traces) constructed using the P-wave sonic (blue log), the S-wave sonic (red log) and the Vp/Vs (magenta log) is used to apply a velocity stretch before the synthetic is tied with the 2004 PS seismic volume (red/black seismic traces).

Time structure maps were created through interpretation for the 5 horizons of interest for both the baseline and monitor surveys. Analysis of these horizons, the seismic volumes and the geological information conveyed by Boyd (Personal Communication) suggests that fractures could be the cause of the low velocity anomaly in the centre of the study area, the extent of which is shown as a "push down" (an increase in travel-time) in Figure 9. In both PP volumes, the low velocity anomaly also exhibits itself as an overall

reduction in seismic amplitude (Figure 10), in the PS volumes however, the seismic amplitudes are unaffected.
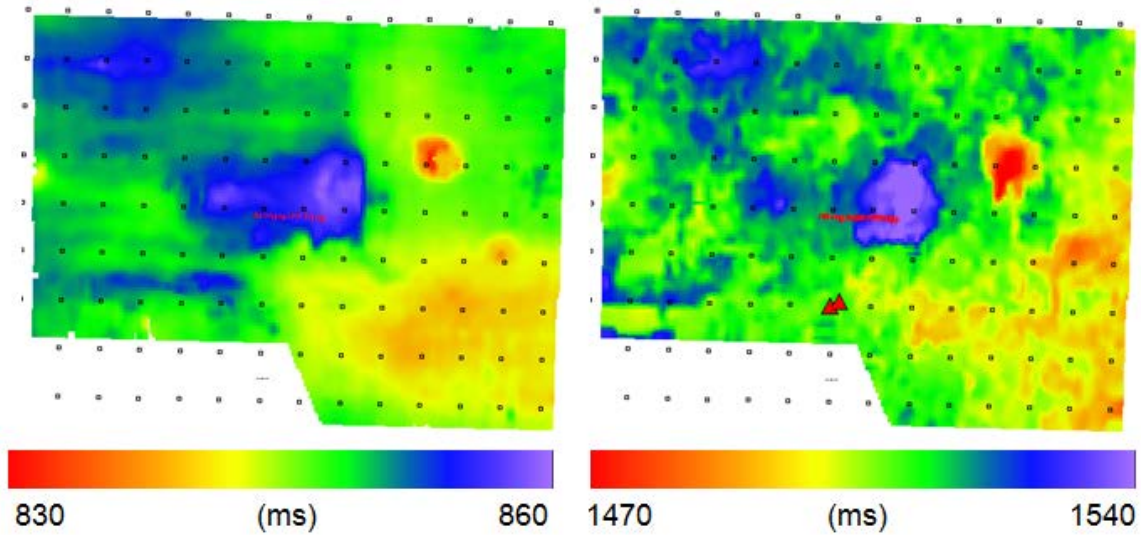

FIG. 9. A time structure map showing the Winnipegosis Formation from the 2004 PP seismic volume (left) and 2004 PS seismic volume (right). The large blue-purple anomaly in the centre of the map shows a travel-time "push down" which is thought to be attributed to the presence of fractures in the carbonate layers above the Prairie Evaporite Formation. The red circle in the Northeast corresponds with an interpreted pinnacle reef, and the yellow-red in the Southeast shows the outline of an interpreted carbonate mound.
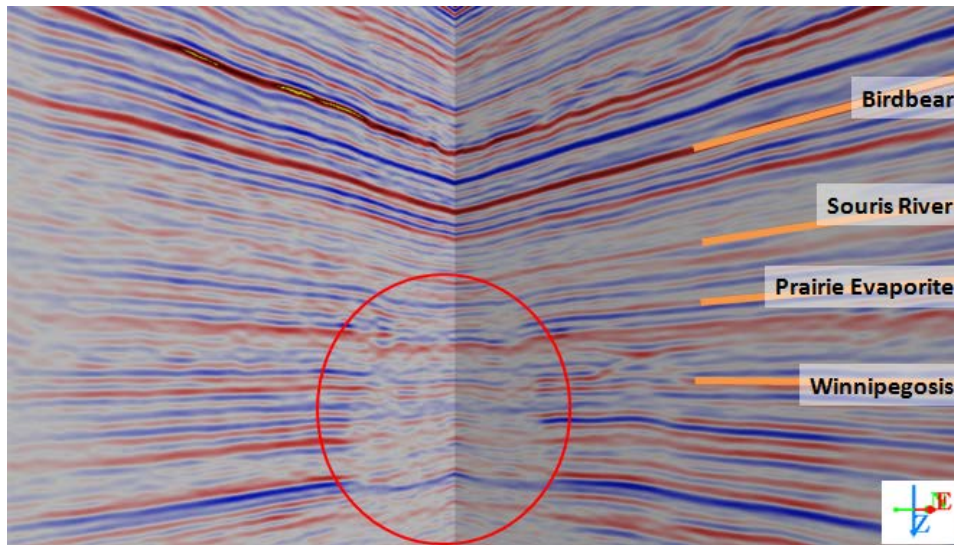

FIG. 10. An inline and crossline from the 2004 PP volume displaying the low amplitude, low velocity anomaly at the centre of the study area (red circle). The anomaly propagates below the Souris River Formation to the bottom of the section.

The PS dataset has a lower frequency content, and is noisier than the PP dataset. As a result, the PS horizons were much more difficult to pick than the PP horizons. However, the use of azimuthal travel-time analysis for both the PP and PS seismic volumes was applied to investigate the presence of seismic anisotropy in the subsurface.

PP Travel-time Analysis

The Souris River Formation shows minimal travel-time differences that are between -5 and 5 ms in the 2004 and 2008 PP volumes (Figures 11 and 12). There are few major differences between the 2004 and 2008 vintages, which speaks to the survey repeatability. The Prairie Evaporite PP time difference plots shows evidence of the mine workings southeast of the study area in the 0&180-90&270 plots (Figure 13).
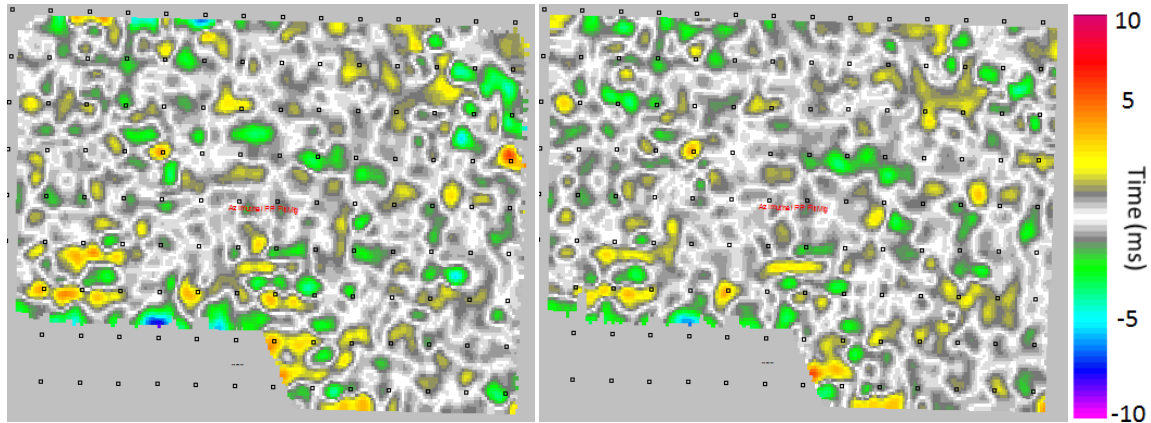

FIG. 11. PP time difference plots for the Souris River Formation calculated by subtracting the 0&180-90&270 azimuths for the 2004 (left) and 2008 (right) seismic volumes.
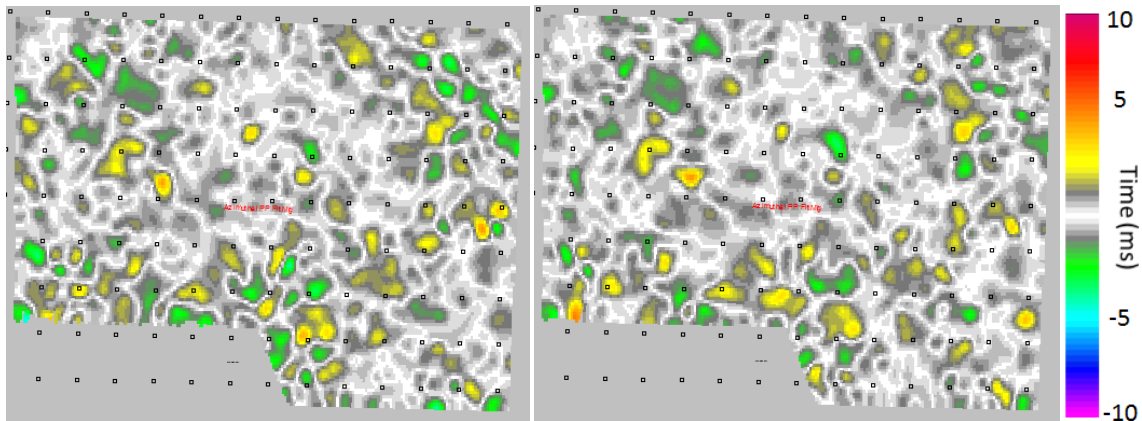

FIG. 12. PP time difference plots, for the Souris River Formation, calculated by subtracting the 45&225-135&315 azimuths for the 2004 (left) and 2008 (right) seismic volumes.

The large negative travel-time difference in the southwest of the survey area is attributed to mine workings in the 90&270 direction which creates a reduction in seismic velocity due to the open mine rooms with the same orientation. The 2008 0&180-90&270 azimuthal PP time difference plot also shows a travel-time difference of +7 ms towards the centre of the study area. The 45&225-135&315 plots (Figure 14) show much less detail because of the trend of the mine workings. The large negative anomaly in the centre of the study area is at the eastern-most edge of the workings which trend east to west. Overall there are minimal travel-time differences between the baseline and monitor surveys in the 45&225-135&315 azimuthal time difference plots.
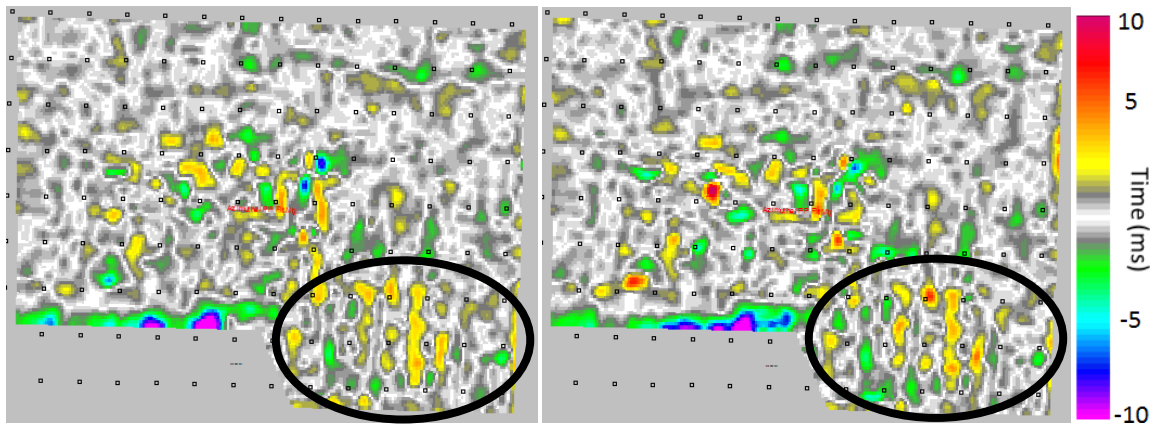
FIG. 13. The 2004 (left) and 2008 (right) 0&180-90&270 azimuth PP time difference plots for the Prairie Evaporite Formation, showing mine workings in the southeast corner of the map (black circle).
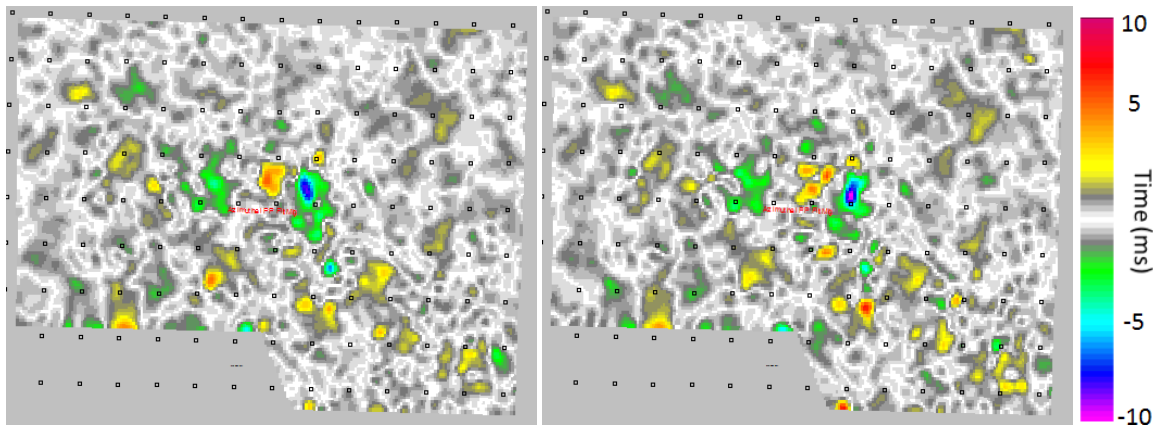

FIG. 14. The 2004 (left) and 2008 (right) 45&225-135&315 azimuth PP time difference plots for the Prairie Evaporite Formation.

The PP time difference plots calculated from the Winnipegosis horizons from the difference azimuths show much larger variations in travel time between orthogonal azimuths, specifically in the central section of the study area. The main anomalies of interest are as large as +10 ms. The southernmost positive differences in the 0&180-90&270 plot (Figure 15) indicates a slow north-south velocity, which if created by fractures, suggest that the fractures trend in an east-west orientation. The western positive travel-time anomaly increases in magnitude between the 2004 and 2008 vintages. The northeastern positive anomaly is connected with the most southeastern anomaly at the easternmost edge of the mine workings in the centre of the study area. Just beyond the eastern edge of mine workings, a negative travel-time anomaly is present, albeit much larger in amplitude in the monitor survey (black ellipses).

In the 45&225-135&315 Winnipegosis PP time difference plots (Figure 16), the most positive travel-time anomaly corresponds with a large, positive travel-time anomaly from the 0&180-90&270 Winnipegosis time difference plots (black circles). The blue negative anomaly towards the west of the central anomaly is located in the centre of the mine workings.
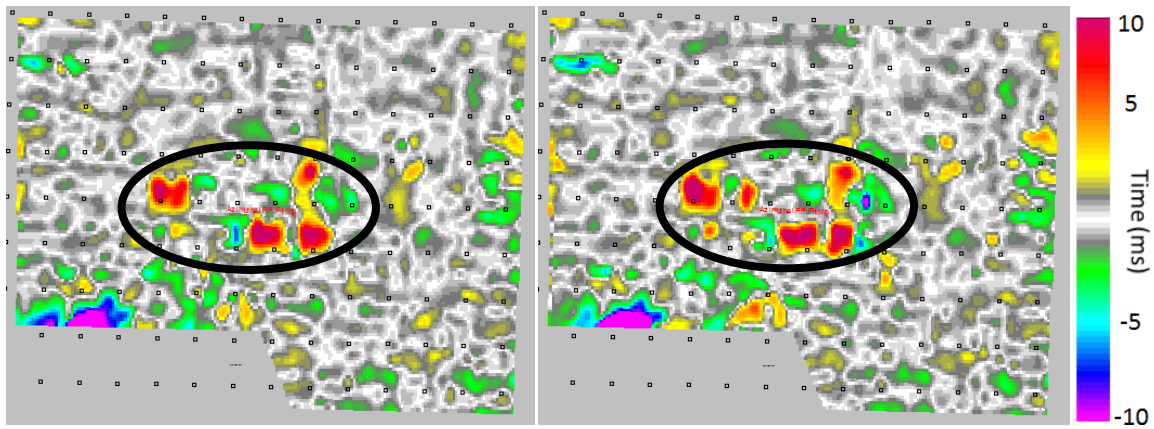
FIG. 15. The 2004 (left) and 2008 (right) 0&180-90&270 azimuth PP time difference plots for the Winnipegosis Formation.
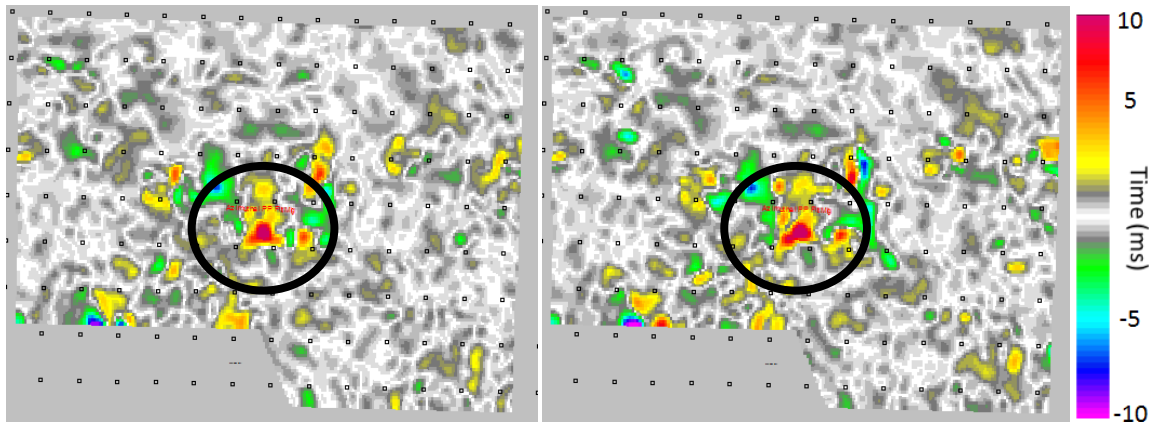

FIG. 16. The 2004 (left) and 2008 (right) 45&225-135&315 azimuth PP time difference plots for the Winnipegosis Formation.

PS Travel-time Analysis

The range of travel-time differences calculated using the PS horizons, as expected, is significantly larger than the travel-time differences calculated from the PP horizons. As in the PP time difference plots, the Souris River horizons do not produce any significant anomalies, they do however, so a much more uniform negative overall difference in the 0&180-90&270 azimuths (Figure 17). There also appear to be some differences in travel-time between the 2004 and 2008 PP time difference plots which have a good correlation to the east of the study area, but not in the west, similar to the 45&225-135&315 azimuth PP time difference plots (Figure 18).
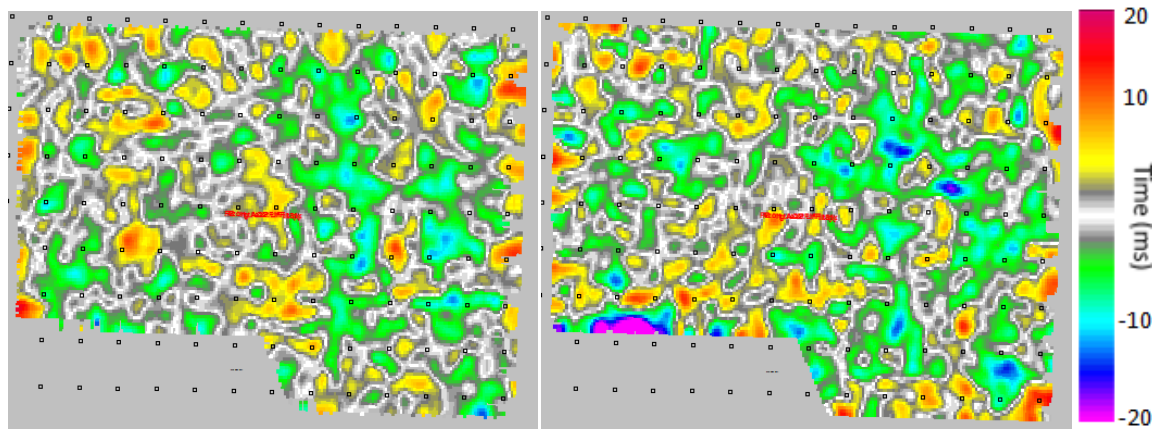
FIG. 17. The 2004 (left) and 2008 (right) 0&180-90&270 azimuth PS time difference plots for the Souris River Formation.
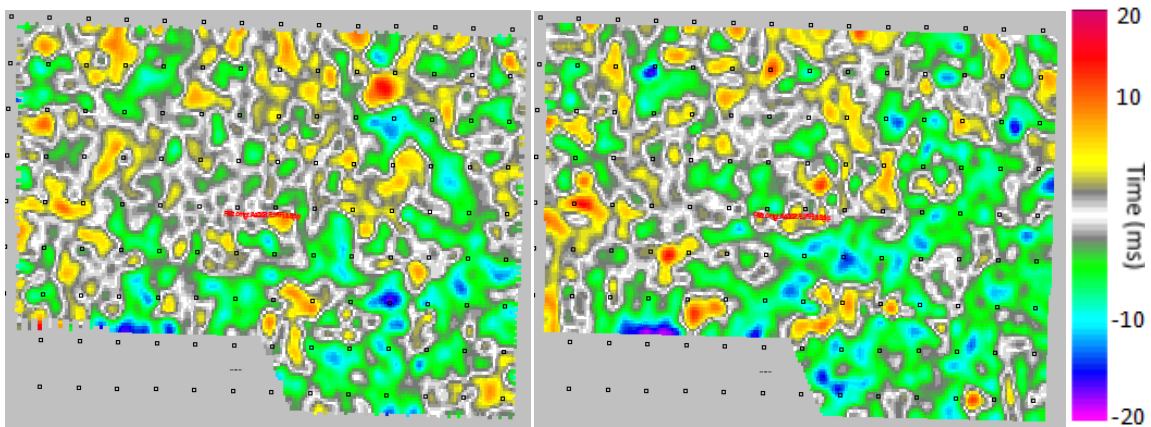

FIG. 18. The 2004 (left) and 2008 (right) 45&225-135&315 azimuth PS time difference plots for the Souris River Formation.

The 2008 Prairie Evaporite 0&180-90&270 azimuth PS time difference plot (Figure 19) shows a large negative travel-time difference, which was not present in the 2004 PS time difference plot (black circle). This indicates a seismic velocity reduction in the 90&270 orientation towards the eastern edge of the central mine workings. The large negative travel-time differences on the eastern edge of the survey increase in magnitude between the baseline and monitor survey, where mine workings line the outermost edges of the survey area. This increased travel-time anomaly could be a result of subsurface stress changes brought on by the presence of the mine room, creating fractures parallel to the 0&180 oriented mine rooms and thus reducing the velocity in the 90&270 orientation. This is supported by the reduced magnitude of the travel-time anomaly in the 45&225-135&315 azimuth PS time difference plots (Figure 20). Although a slight increase in negative travel-time difference is present where some 0&180 aligned mine workings intersect those at a 90&270 orientation (centre of eastern edge of survey).
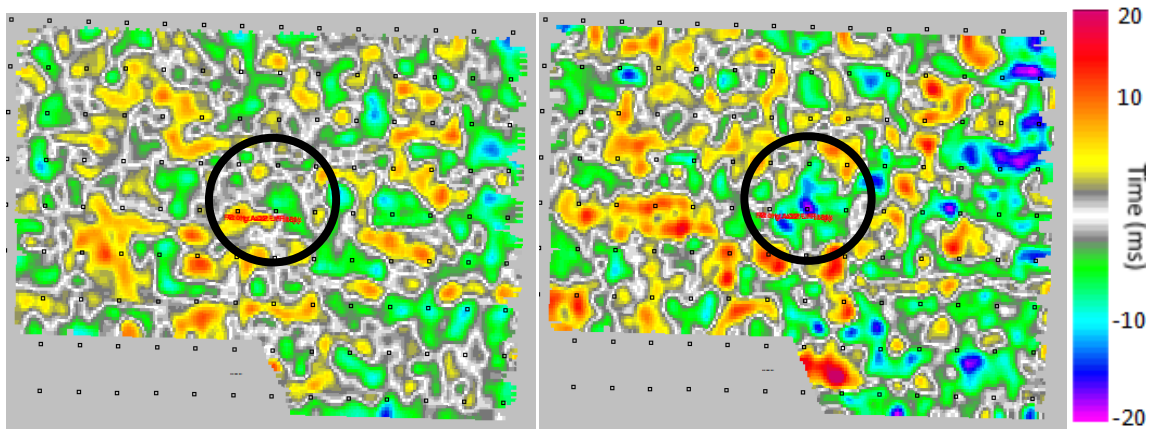
FIG. 19. The 2004 (left) and 2008 (right) 0&180-90&270 azimuth PS time difference plots for the Prairie Evaporite Formation. The black circle indicates a large negative travel-time difference in the 2008 volume, not present in 2004.
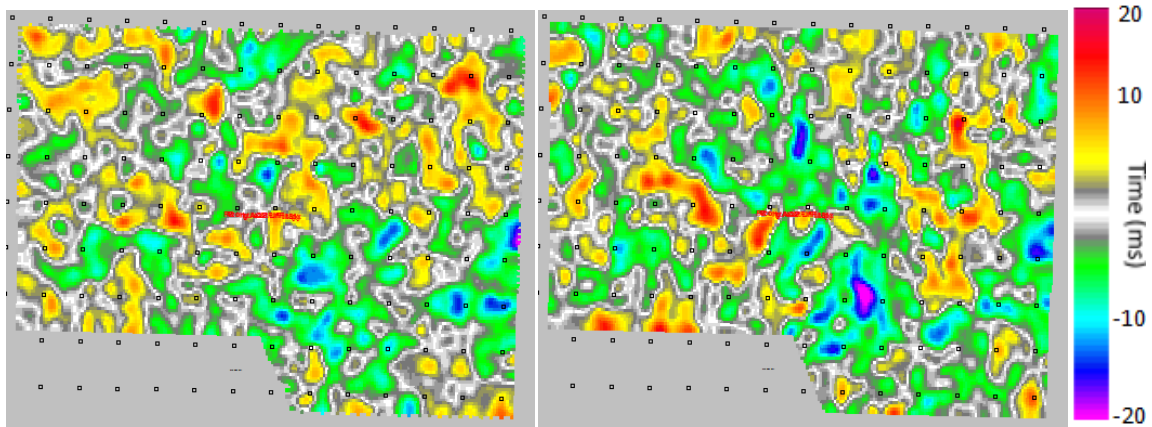

FIG. 20. The 2004 (left) and 2008 (right) 45&225-135&315 azimuth PS time difference plots for the Prairie Evaporite Formation. The black circle indicates a large negative travel-time difference in the 2008 volume, not present in 2004.

The Winnipegosis Formation shows a high positive travel-time anomaly on the west side of the 2004 0&180-90&270 azimuth PS time difference plot (Figure 21), which is not present in the corresponding 2008 map. The largest positive and negative anomalies in the centre of the dataset correspond to the edges of the central mine workings, furthermore the orientation of slow seismic wave propagation in the PS time difference plots are identical to those in the PP time difference plots (Figure 15). The travel-time anomalies in the northeast of the 2004 0&180-90&270 azimuth time difference plot are in the area of the interpreted pinnacle reef, where the Winnipegosis reef in the 0&180 volume appears wider than in the 90&270 volume creating a negative travel-time difference on the edges of the interpreted reef. The 45&225-135&315 azimuth time difference plots (Figure 22) show an increase in the positive anomaly to the east of the central mine workings in the monitor survey which is not present in the baseline survey. The 2008 survey also sees an increase in the negative anomaly in the southeast of the study area.
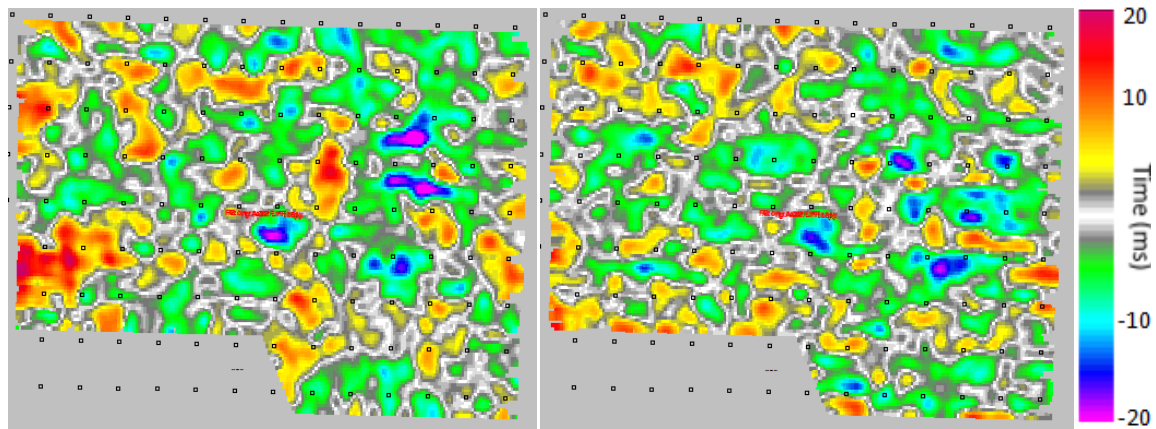
FIG. 21. The 2004 (left) and 2008 (right) 0&180-90&270 azimuth PS time difference plots for the Winnipegosis Formation.
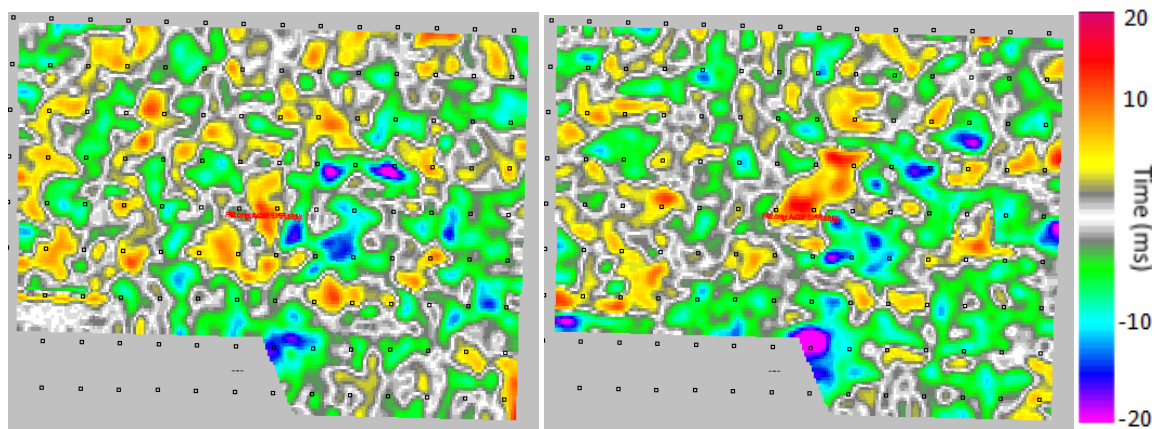

FIG. 22. The 2004 (left) and 2008 (right) 45&225-135&315 azimuth PS time difference plots for the Winnipegosis Formation.

VP/VS ANALYSIS

Where fractures are present in the subsurface, the Vp/Vs will increase depending on fracture density because the P-wave velocity will decrease less substantially than the S-wave velocity (Hardage, DeAngelo, Murray, & Sava, 2011; O'Connell & Budiansky, 1974). In order to determine the relative extent of fracturing in the subsurface, analysing the Vp/Vs for significant increases is done using the picked horizons from the PP and PS volumes. In order to visualize the vertical changes in Vp/Vs throughout a seismic volume, horizon matching is performed whereby travel-times associated with each point of a PS horizon shifted to match that of the corresponding PP horizon. Using Equation 1, the Vp/Vs is calculated and a crossline showing how Vp/Vs changes after the application of the horizon matching process is displayed in Figure 23.

$$\frac{V_P}{V_S} = \frac{2\Delta t_{ps} - \Delta t_{pp}}{\Delta t_{pp}} \tag{1}$$

Where Vp is the P-wave velocity, Vs is the S-wave velocity, dts is the PS travel-time and dtp is the P-wave travel-time.

Where well control is present, Vp/Vs is within reasonable values for carbonates (Palaz & Marfurt, 1997; Mavko, 2005).
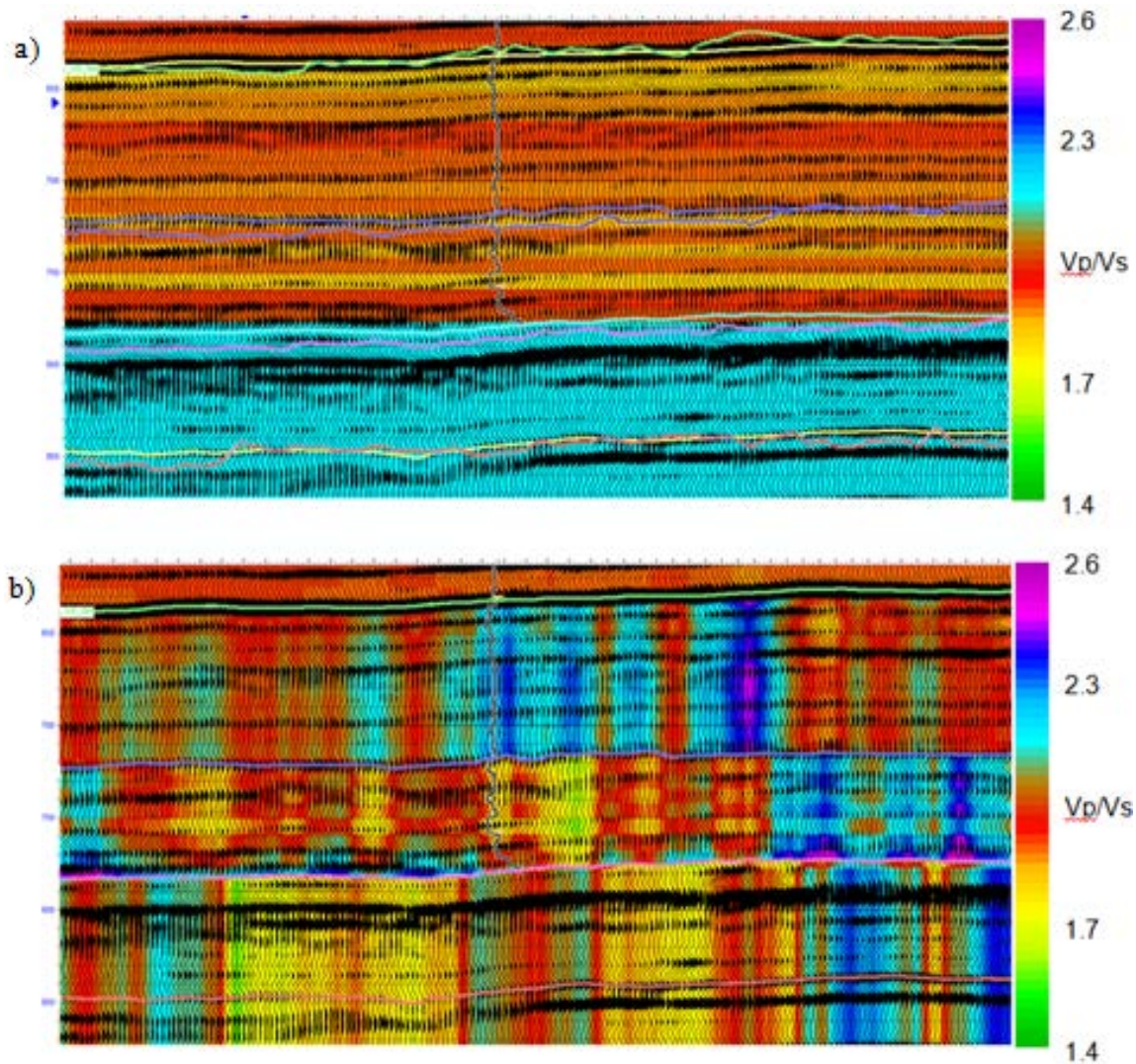

FIG. 23. Crossline through one of the wells containing a dipole sonic log. Vp/Vs, shown in color, a) is strictly based on the contributions of the Vp/Vs calculated from the ratio of the P-wave to S-wave sonic logs, where b) Vp/Vs post-horizon matching. The 2004 vertical component full azimuth stack seismic volume is shown as wiggle traces. The well log shown is the calculated Vp/Vs with values ranging from 1.7-2.2.

For the stratigraphy below the depth of well penetration, Vp/Vs at the bottom of the well is propagated to the base of the volume (cyan color at the bottom of the section in Figure 23a). The increase from an average Vp/Vs of 1.9, in the upper section of Figure 23a, to a Vp/Vs of 2.2 is present because of a large reduction in shear wave velocity at the base of the well log interval. As there is also a decrease in the P-wave velocity, this spike has been interpreted to be the result of fracturing within the Dawson Bay Formation. When the horizon matching workflow is applied, Vp/Vs is altered based on PP and PS travel-times for the particular horizons used. In Figure 23b, the effects of applying the horizon matches for the Birdbear, Souris River, Prairie Evaporite and Winnipegosis formations

can be seen for a crossline through a well with a dipole sonic log. Vp/Vs increases after the horizon matching is applied. The vertical streaking seen is a function of the difficulties associated with picking the horizons on the PS seismic volumes, and the Vp/Vs calculated is then combined with the log calculated Vp/Vs to produce the Vp/Vs on the crossline. Figure 24 shows a crossline through the low velocity, low amplitude anomaly in the centre of the seismic volume. Vp/Vs in the upper section is relatively unchanged from those values seen outside of the anomaly, however, the Dawson Bay Formation exhibits a significant increase in Vp/Vs, with values approaching 2.6 where the seismic anomaly is present.
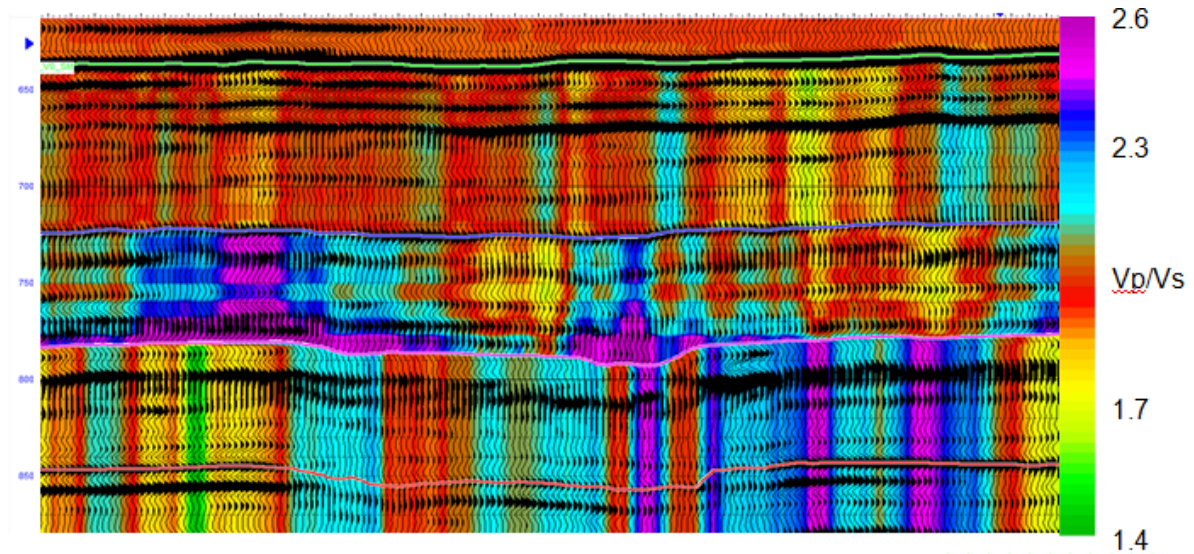

FIG. 24. Crossline from the 2004 seismic volume through the low velocity anomaly in the centre of the seismic volume. Notice the significant change of Vp/Vs relative to the crossline in Figure 23, specifically the increase in the centre of the line just above the Prairie Evaporite horizon.

The 2008 seismic volumes show a similar Vp/Vs pattern as the 2004 volumes which have had horizon matching applied. Figure 25a shows Vp/Vs calculated using the 2008 horizons and can be compared to the crossline in Figure 23b. The largest difference occurs just above the Prairie Evaporite horizon within the Dawson Bay Formation where Vp/Vs in 2008 is consistently in the 2.3-2.6 range. Figure 25b shows the 2008 crossline which is equivalent to the line in Figure 24. The major difference here is that the 2008 data does not show the high Vp/Vs of 2.6 in the East which propagates up through the section from the Dawson Bay Formation, but rather stays between 2.0 and 2.3. The 2008 section shows a much more laterally continuous region of high Vp/Vs at the base of the Dawson Bay Formation, which could be attributed to the existence of additional fracturing in the area.

In order to better constrain the lateral continuity of the Vp/Vs, the interval Vp/Vs through the section was analysed. The interval Vp/Vs is computed using the PP and PS travel-times at the top and base of the targeted region. Figures 26-28 show the interval Vp/Vs corresponding to the Birdbear Formation-Souris River Formation, Souris River Formation-Prairie Evaporite Formation and Prairie Evaporite Formation-Winnipegosis Formation sequences for the 2004 and 2008 seismic vintages.
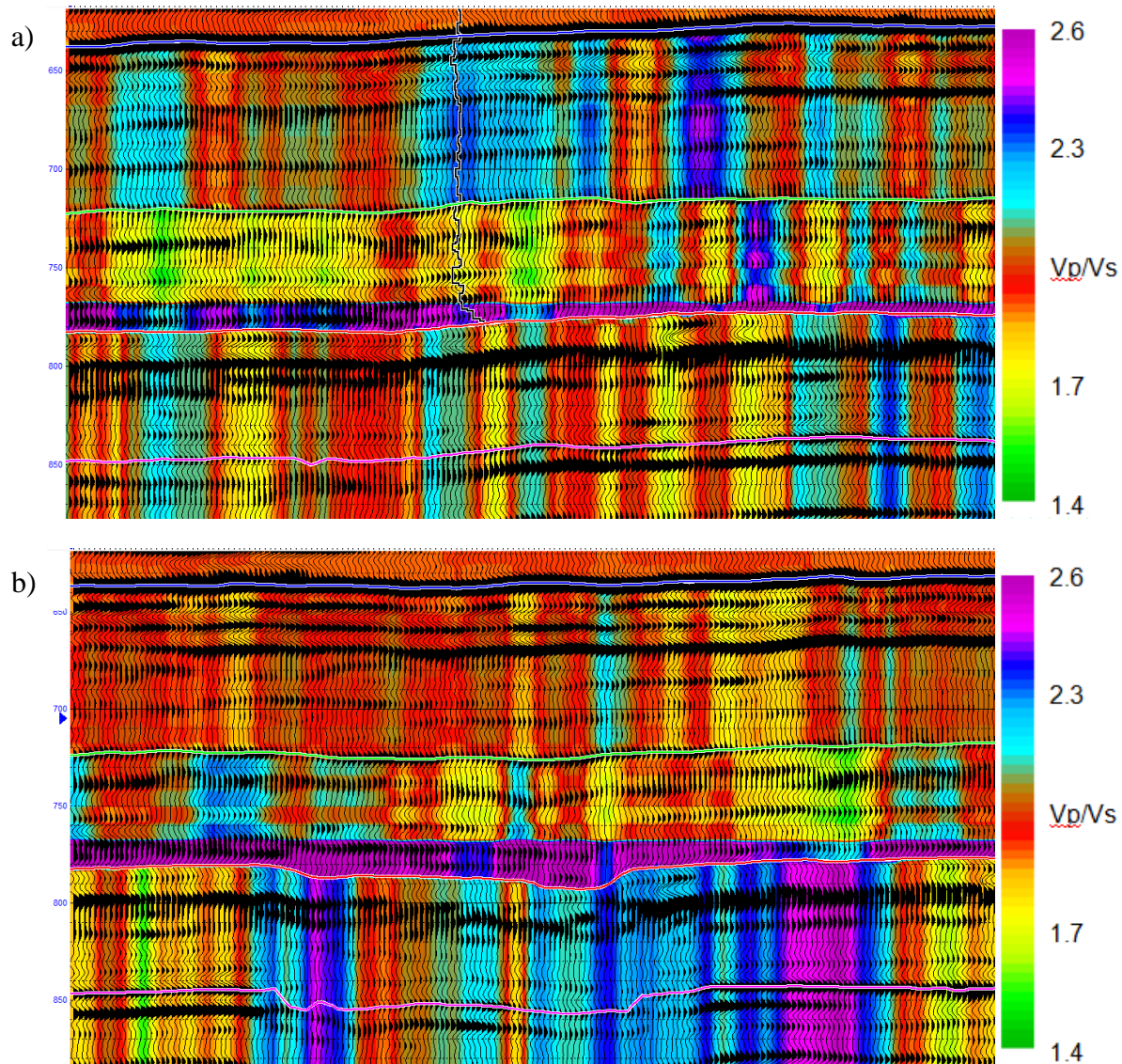
FIG. 25. Two crosslines showing the Vp/Vs calculated through the horizon matching process. a) the crossline through the reference well used in Figure 23; b) the 2008 crossline that matches the 2004 crossline from Figure 24.

A comparison of the interval Vp/Vs between the Birdbear and Souris River horizons (Figure 26) confirms that there is little difference in the seismic volumes above the Souris River Formation between 2004 and 2008. Furthermore, the Vp/Vs for the interval is reasonable for the carbonate stratigraphy with an average Vp/Vs of 2.0 and local minimum and maximum values of 1.75 and 2.4, respectively. The Vp/Vs from the fractured interval between the Souris River and Prairie Evaporite formations (Figure 27) displays a higher average Vp/Vs of 2.2 than found in the Birdbear-Souris River succession. Specifically, the higher average values can be found in the west and southeast of the study area, areas where mine workings are present in the Prairie Evaporite Formation. The northeast exhibits a lower average Vp/Vs of approximately 1.8, which corresponds to the areas where fractures would not be stimulated due to mine workings. Neither the Birdbear-Souris River, nor the Souris River-Prairie Evaporite interval Vp/Vs

plots show any significant differences between the 2004 and 2008 vintages, indicating that no new fractures were formed within the Dawson Bay Formation during the time between the baseline and monitor surveys.

The interval Vp/Vs for the Prairie Evaporite-Winnipegosis sequence between 2004 and 2008 shows some significant differences between vintages. Most notable are the significant decrease of Vp/Vs in the southwest of the study area and the increase of Vp/Vs from 2.1-2.6. These discrepancies require further analysis in order to determine the geological cause. Two anomalies, however, remain constant over both vintages: the pinnacle reef in the northeast (low Vp/Vs of approximately 1.4) and the Vp/Vs high of 2.6 in the centre of the dataset where the low amplitude anomaly is located, supporting the hypothesis that fractures are responsible for the presence of the low velocity anomaly.
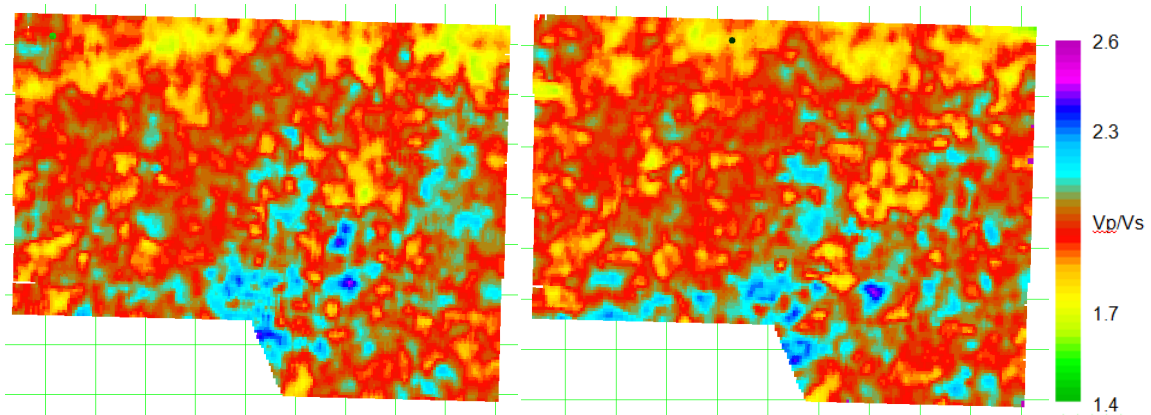

FIG. 26. Interval Vp/Vs for the 2004 (left) and 2008 (right) Birdbear and Souris River formations.
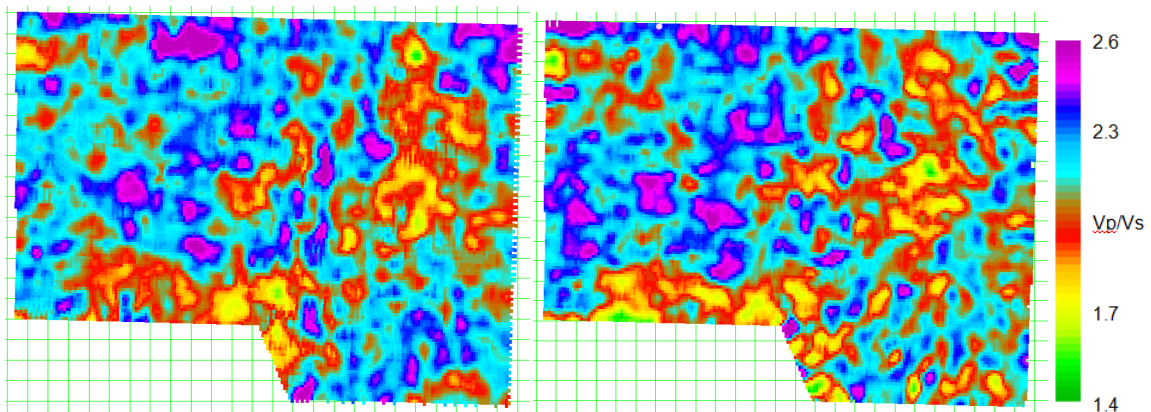

FIG. 27. Interval Vp/Vs for the 2004 (left) and 2008 (right) Souris River and Prairie Evaporite formations.
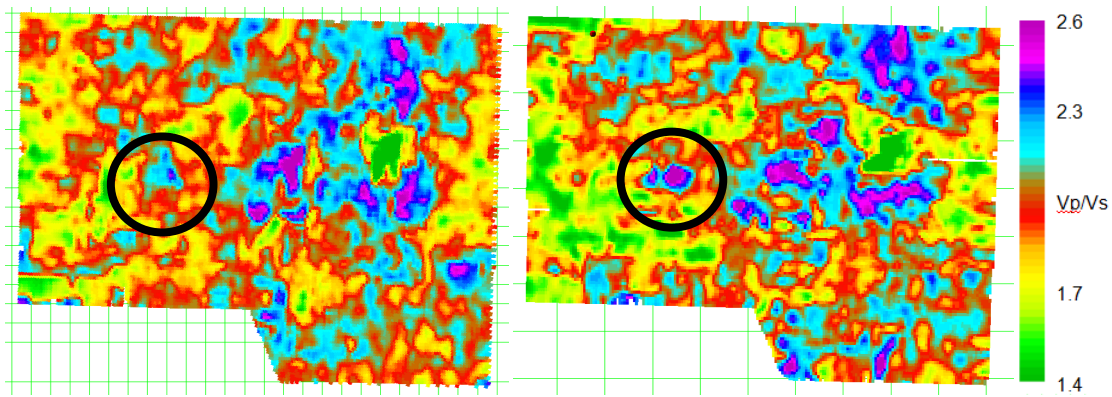
FIG. 28. Interval Vp/Vs for the 2004 (left) and 2008 (right) Prairie Evaporite and Winnipegosis formations. The black circles show an area of significant increase in Vp/Vs between surveys.

SUMMARY

This report utilizes the analysis of azimuthal travel-times from PP and PS seismic volumes by horizon differencing in order to examine the stratigraphy surrounding a potash mine in southeast Saskatchewan, Canada. The goal of this work is to interpret the effect of fractures within the Dawson Bay Formation through the calculation of travel-time differences between seismic events in volumes which are created using a stack of orthogonal source-receiver azimuths. This is made possible because fractures reduce the velocity of seismic waves traveling across the fracture plane, creating a state of HTI, which can be identified due to the increase of event travel-time isolated to the azimuths perpendicular to fracture strike. Interpretation of the time difference plots created from the seismic events picked in the multiple azimuthally sectored PP and PS volumes provides insight into the state of anisotropy in the subsurface.

Analysis of the PP time difference plots shows that fractures with a preferential orientation propagate outwards from the mining operation in a direction parallel to orientation of excavation, specifically below the mine in the Winnipegosis Formation. Above the mine, in the Dawson Bay Formation, the PP time difference plots show a reduction of seismic velocity in the 90&270 direction suggesting that fractures are propagating parallel to the eastern edge of the central mining operation. Although fractures are likely to be present throughout the excavation area, they likely have randomly oriented themselves which creates a reduction of seismic velocity in all directions and therefore is not be visible in the PP time difference plots focusing on orthogonal azimuths of wave propagation. The 2008 PS time difference plots also produced a large negative travel-time anomaly in the Prairie Evaporite Formation 0&180-90&270 sectors, at the edge of the mining area, which was not present in the baseline survey. These observations suggest that there is fracturing surrounding the mine workings which creates HTI, visible through azimuthal travel-time analysis.

An increase in Vp/Vs, calculated using the interpreted PP and PS horizons, corresponds with the low velocity anomaly in the centre of the study area and suggests the presence of fracture networks which extend vertically from the Prairie Evaporite

Formation towards the top of the Dawson Bay Formation. Vp/Vs also increases between the 2004 and 2008 seismic volumes where the central low velocity anomaly is present indicating a potential increase in fracture density through this anomaly over the course of the acquisition of the two seismic surveys.

ACKNOWLEDGEMENTS

REFERENCES

Boyd, J. (2012, 03 12). Personal Communication.

De Mille, G., Shouldice, J. R., & Nelson, H. W. (1964). Collapse Structures Related to Evaporites of the Prairie Formation, Saskatchewan. *Geological Society of America Bulletin* , 307-316.

Douglas, R. J. (1970). *Geology and Economic Minerals of Canada.* Ottawa: Geological Survey of Canada.

Fuzesy, L. (1982). Petrology of Potash Ore in the Esterhazy Member of the Middle Devonian Prairie Evaporite in Southeastern Saskatchewan. *Proceedings of the 4th International Williston Basin Symposium*, (pp. 67-73).

Hardage, B., DeAngelo, M. V., Murray, P., & Sava, D. (2011). *Rock Physics.* Tulsa, OK: Society of Exploration Geophysicists.

Hudson, J. (1981). Wave Speeds and Attenuation of Elastic Waves in Material Containing Cracks. *Geophysical Journal of the Royal Astronomical Society* , 133-150.

Lynn, H. B., Beckham, W., Simon, K., Bates, C. R., Layman, M., & Jones, M. (1999). P-wave and S-wave azimuthal anisotropy at a naturally fractured gas reservoir, Bluebell-Altamont Field, Utah. *Geophysics* , 1312-1328.

Mavko, G. (2005, 03 26). *Conceptual Overview of Rock and Fluid Factors that Impact Seismic Velocity and Impedance*. Retrieved 11 11, 2012, from Stanford Rock Physics Laboratory: https://pangea.stanford.edu/courses/gp262/Notes/8.SeismicVelocity.pdf

Mossop, G. D., & Shetsen, I. (1993). *Geological Atlas of the Western Canada Sedimentary Basin.* Canadian Society of Petroleum Geologists/Alberta Research Council.

O'Connell, R., & Budiansky, B. (1974). Seismic Velocity in Dry and Saturated Cracked Solids. *Journal of Geophysical Research* , 5412-5426.

Palaz, I., & Marfurt, K. J. (1997). *Carbonate Seismology.* Tulsa, OK: Society of Exploration Geophysicists.

Ruger, A. (1997). P-wave Reflection Coefficients for Transversly Isotropic Models with Vertical and Horizontal Axis of Symmetry. *Geophysics* , 713-722.

Thomsen, L. (1986). Weak Elastic Anisotropy. *Geophysics* , 1954-1966.

Tsvankin, I. (1997). Reflectiong Moveout and Parameter Estimation for Horizontal Transverse Isotropy. *Geophysics* , 614-629.

Warren, J. K. (2006). *Evaporites: Sediments, Resources and Hydrocarbons.* Berlin: Springer.

Zhang, Z. (2010). *Assessing attenuation, fractures, and anisotropy using logs, vertical seismic profile, and three-component seismic data: heavy oilfield and potash mining examples.* Calgary: The University of Calgary.
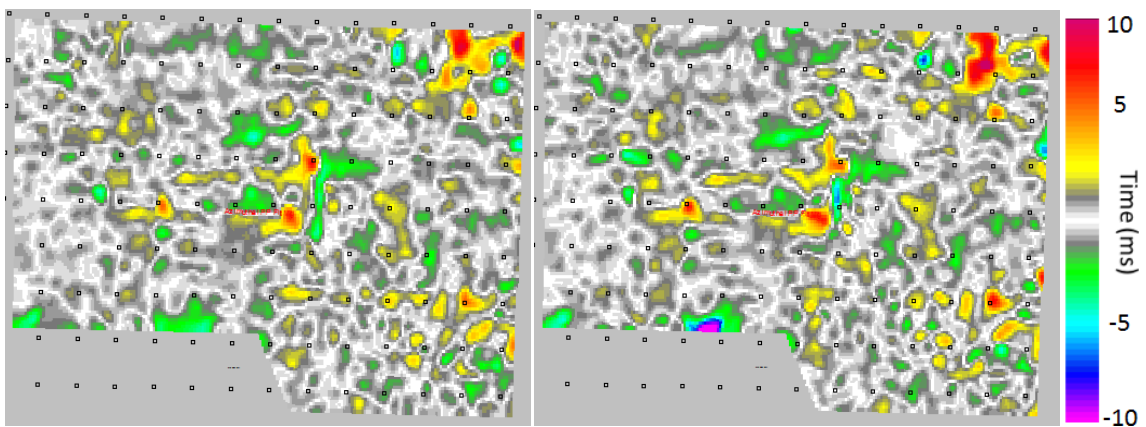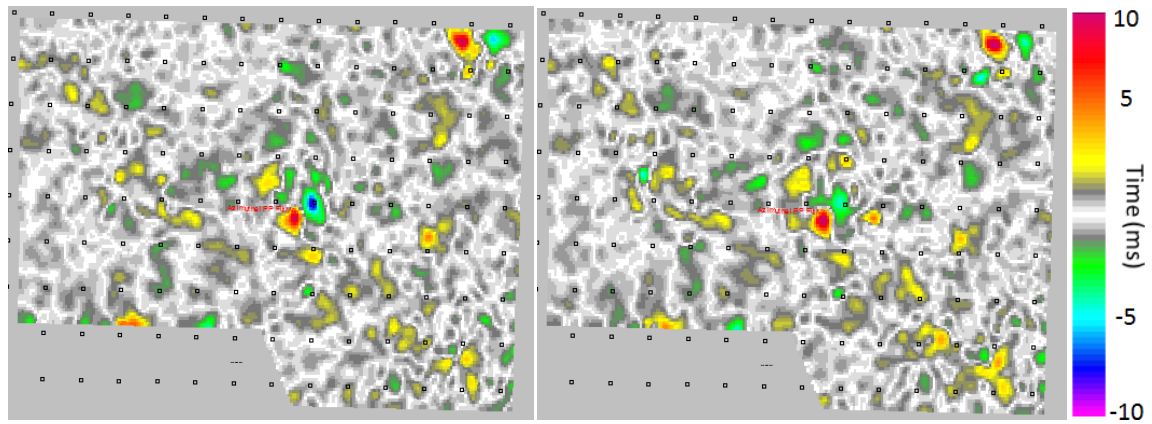
APPENDIX
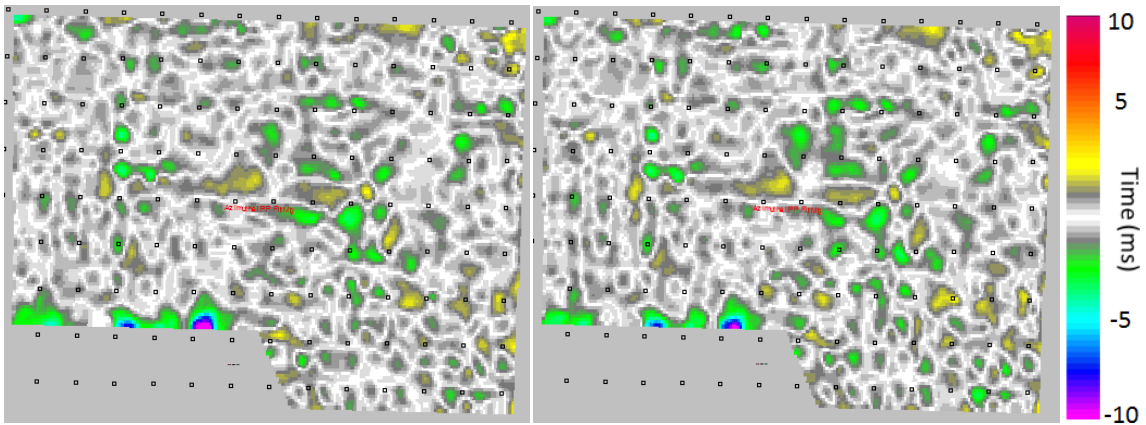
A. 1. The 2004 (left) and 2008 (right) PP, 0&180-90&270 azimuth PP time difference plots for the Birdbear Formation.
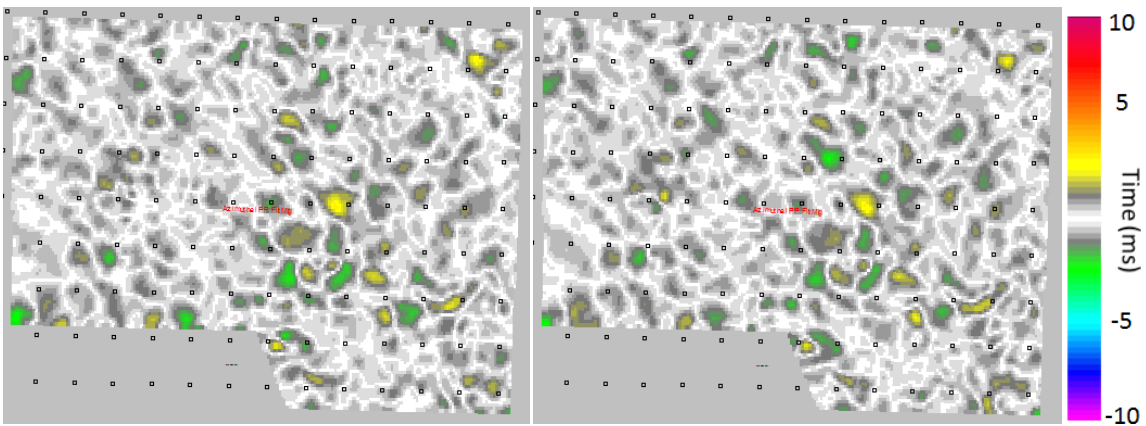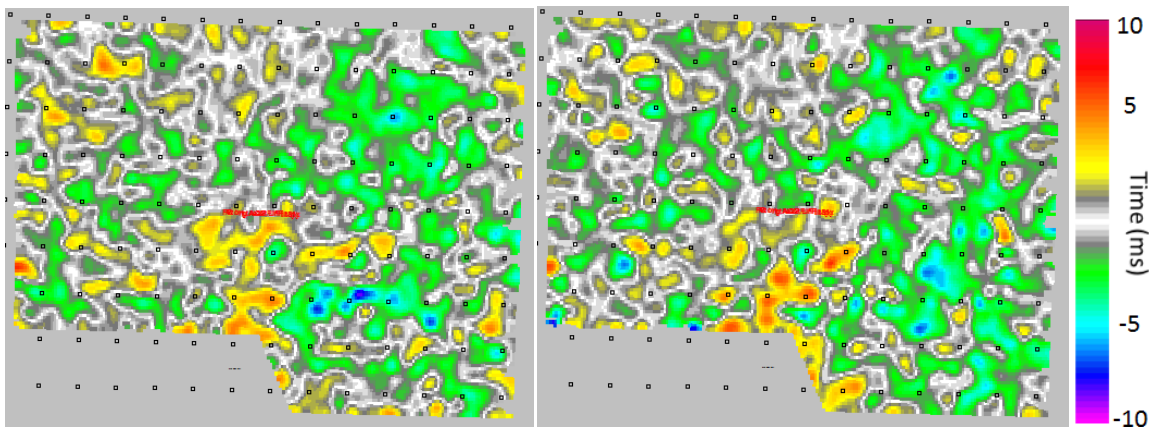

A. 2. The 2004 (left) and 2008 (right) PP, 45&225-135&315 azimuth PP time difference plots for the Birdbear Formation.
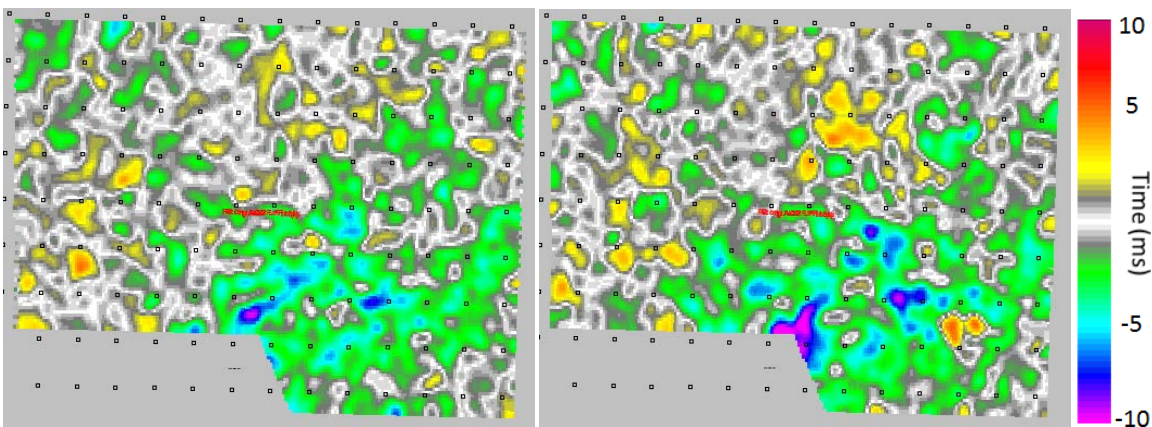

A. 3. The 2004 (left) and 2008 (right) PP, 0&180-90&270 azimuth PP time difference plots for the Dawson Bay Formation.
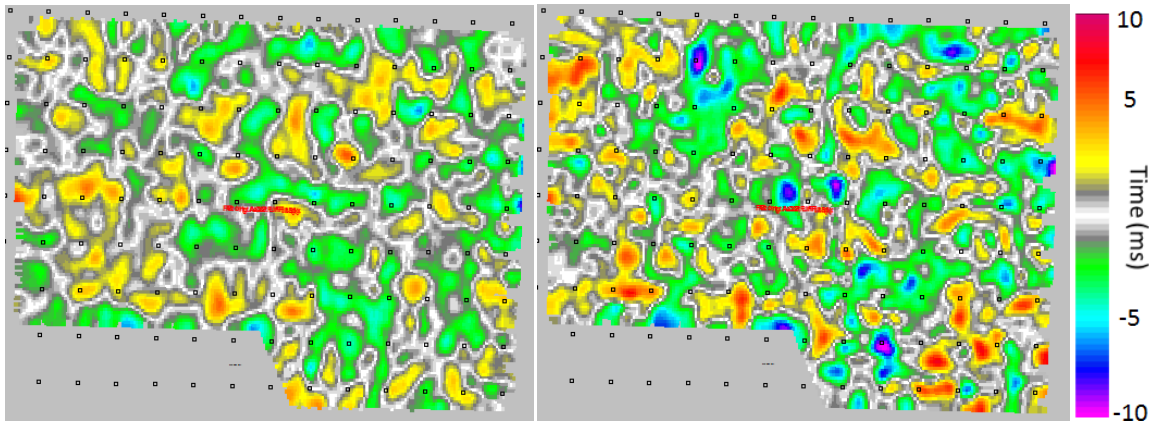
A. 4. The 2004 (left) and 2008 (right) PP, 45&225-135&315 azimuth PP time difference plots for the Dawson Bay Formation.
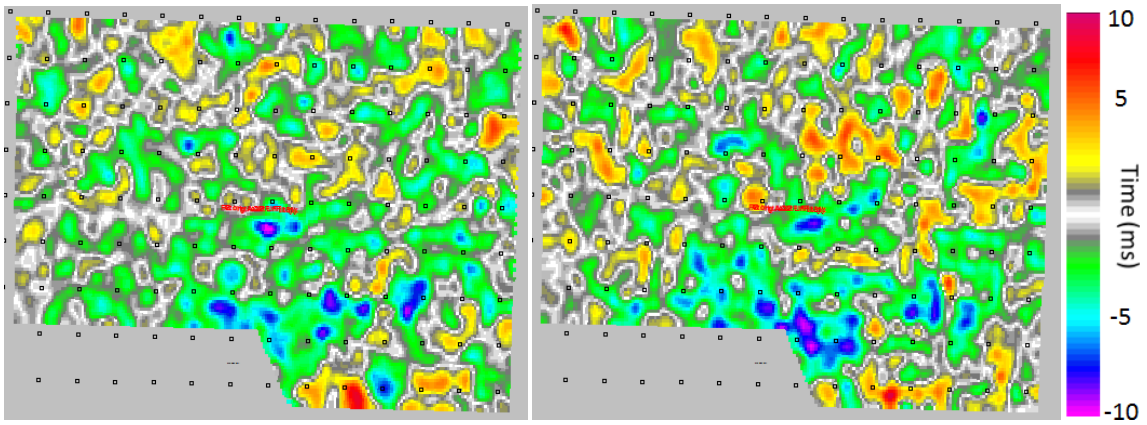

A. 5. The 2004 (left) and 2008 (right) PS, 0&180-90&270 azimuth PS time difference plots for the Birdbear Formation.

A. 6. The 2004 (left) and 2008 (right) PP, 45&225-135&315 azimuth PS time difference plots for the Birdbear Formation.

A. 7. The 2004 (left) and 2008 (right) PP, 0&180-90&270 azimuth PS time difference plots for the Dawson Bay Formation.

A. 8. The 2004 (left) and 2008 (right) PP, 45&225-135&315 azimuth PS time difference plots for the Dawson Bay Formation.